1521-009X/46/7/1030–1040$35.00
Drug Metabolism and Disposition
U.S. Government work not protected by U.S. copyright

https://doi.org/10.1124/dmd.117.080176
Drug Metab Dispos 46:1030–1040, July 2018

Structure-Activity Relationships of the Main Bioactive Constituents of *Euodia rutaecarpa* on Aryl Hydrocarbon Receptor Activation and Associated Bile Acid Homeostasis[S]

Youbo Zhang,[1] Tingting Yan,[1] Dongxue Sun, Cen Xie, Yiran Zheng, Lei Zhang, Tomoki Yagai, Kristopher W. Krausz, William H. Bisson, Xiuwei Yang, and Frank J. Gonzalez

Laboratory of Metabolism, Center for Cancer Research, National Cancer Institute, National Institutes of Health, Bethesda, Maryland (Yo.Z., Ti.Y., D.S. C.X., To.Y., K.W.K., F.J.G.); State Key Laboratory of Natural and Biomimetic Drugs and Department of Natural Medicines, School of Pharmaceutical Sciences, Peking University, Beijing, China (Yo.Z., Yi.Z., L.Z., X.Y.); Department of Environmental and Molecular Toxicology, Oregon State University, Corvallis, Oregon (W.H.B.); and College of Traditional Chinese Medicine, Shenyang Pharmaceutical University, Shenyang, Liaoning, China (D.S.)

Received January 5, 2018; accepted April 19, 2018

ABSTRACT

Rutaecarpine (RUT), evodiamine (EOD), and dehydroevodiamine (DHED) are the three main bioactive indoloquinazoline alkaloids isolated from *Euodia rutaecarpa*, a widely prescribed traditional Chinese medicine. Here, the structure-activity relationships of these analogs for aryl hydrocarbon receptor (AHR) activation were explored by use of *Ahr*-deficient (*Ahr*$^{-/-}$) mice, primary hepatocyte cultures, luciferase reporter gene assays, in silico ligand-docking studies, and metabolomics. In vitro, both mRNA analysis of AHR target genes in mouse primary hepatocytes and luciferase reporter assays in hepatocarcinoma cell lines demonstrated that RUT, EOD, and DHED significantly activated AHR, with an efficacy order of RUT > DHED > EOD. Ligand-docking analysis predicted that the methyl substitute at the N-14 atom was a key factor affecting AHR activation. In vivo, EOD was poorly orally absorbed and failed to activate AHR, whereas RUT and DHED markedly upregulated expression of the hepatic AHR gene battery in wild-type mice, but not in *Ahr*$^{-/-}$ mice. Furthermore, RUT, EOD, and DHED were not hepatotoxic at the doses used; however, RUT and DHED disrupted bile acid homeostasis in an AHR-dependent manner. These findings revealed that the methyl group at the N-14 atom of these analogs and their pharmacokinetic behaviors were the main determinants for AHR activation, and suggest that attention should be given to monitoring bile acid metabolism in the clinical use of *E. rutaecarpa*.

Introduction

The aryl hydrocarbon receptor (AHR), also known as the dioxin receptor, is a member of the basic helix-loop-helix Per-ARNT-Sim (PAS) family of transcription factors that is activated by a wide variety of lipophilic ligands, particularly for those containing at least one aromatic ring (Denison and Heath-Pagliuso, 1998; Hahn, 2002; Abel and Haarmann-Stemmann, 2010; Guyot et al., 2013). Once bound with ligand, the AHR is activated, translocates to the nucleus, and forms a heterodimer with the aryl hydrocarbon nuclear translocator. The heterodimer then binds to xenobiotic response elements in the promoter regions of its target genes to initiate transcription. AHR target genes include phase I and phase II metabolic enzymes and xenobiotic transporters (Köhle and Bock, 2007; Haarmann-Stemmann et al., 2010; Sorg, 2014; Gao et al., 2016). Among these target genes are those encoding the CYP1 family enzymes CYP1A1, CYP1A2, and CYP1B1 that metabolize many xenobiotics, including some AHR ligands (Nebert and Karp, 2008).

AHR is highly inducible by a wide range of exogenous compounds (Fernandez-Salguero et al., 1996; Schmidt et al., 1996; Spink et al., 2015), and its activation could either cause metabolic activation of chemical toxicants and procarcinogens or inactivate xenobiotics (Shimizu et al., 2000; Connor et al., 2008; de Waard et al., 2008; Veldhoen et al., 2009). The biologic effects of various AHR activators vary, thus highlighting the need for determining the structure-activity relationship for AHR and its ligands (Connor et al., 2008; de Waard et al., 2008; Veldhoen et al., 2009). Determining biologic effects among different AHR agonists by use of structure-activity relationships could be a strategy for modeling the ligand-binding site and understanding the mechanism of AHR signaling.

Rutaecarpine (RUT), evodiamine (EOD), and dehydroevodiamine (DHED) are the three major biologic constituents isolated from *Evodia*

This project was supported by the National Cancer Institute Intramural Research Program and the National Natural Science Foundation of China [Grant 81773865].

[1]Yo.Z. and Ti.Y. contributed equally to this work.

The authors declare that they have no conflict of interest.

https://doi.org/10.1124/dmd.117.080176.

[S]This article has supplemental material available at dmd.aspetjournals.org.

ABBREVIATIONS: AHR, aryl hydrocarbon receptor; ALT, alanine aminotransferase; AST, aspartate aminotransferase; BSEP, bile salt export pump; CA, cholic acid; DHED, dehydroevodiamine; DRE, dioxin-response elements; EOD, evodiamine; FBS, fetal bovine serum; FXR, farnesoid X receptor; HB, hydrogen-bonding; 3-MC, 3-methylcholanthrene; α-MCA, α-muricholic acid; β-MCA, β-muricholic acid; ω-MCA, ω-muricholic acid; MS/MS, tandem mass spectrometry; PAS, Per-ARNT-Sim; PCA, principal components analysis; qPCR, quantitative polymerase chain reaction; RUT, rutaecarpine; SHP, small heterodimer partner; TCDD, 2,3,7,8-tetrachlorodibenzo-p-dioxin; T-DCA, taurodeoxycholic acid; UPLC, ultra-performance liquid chromatography.

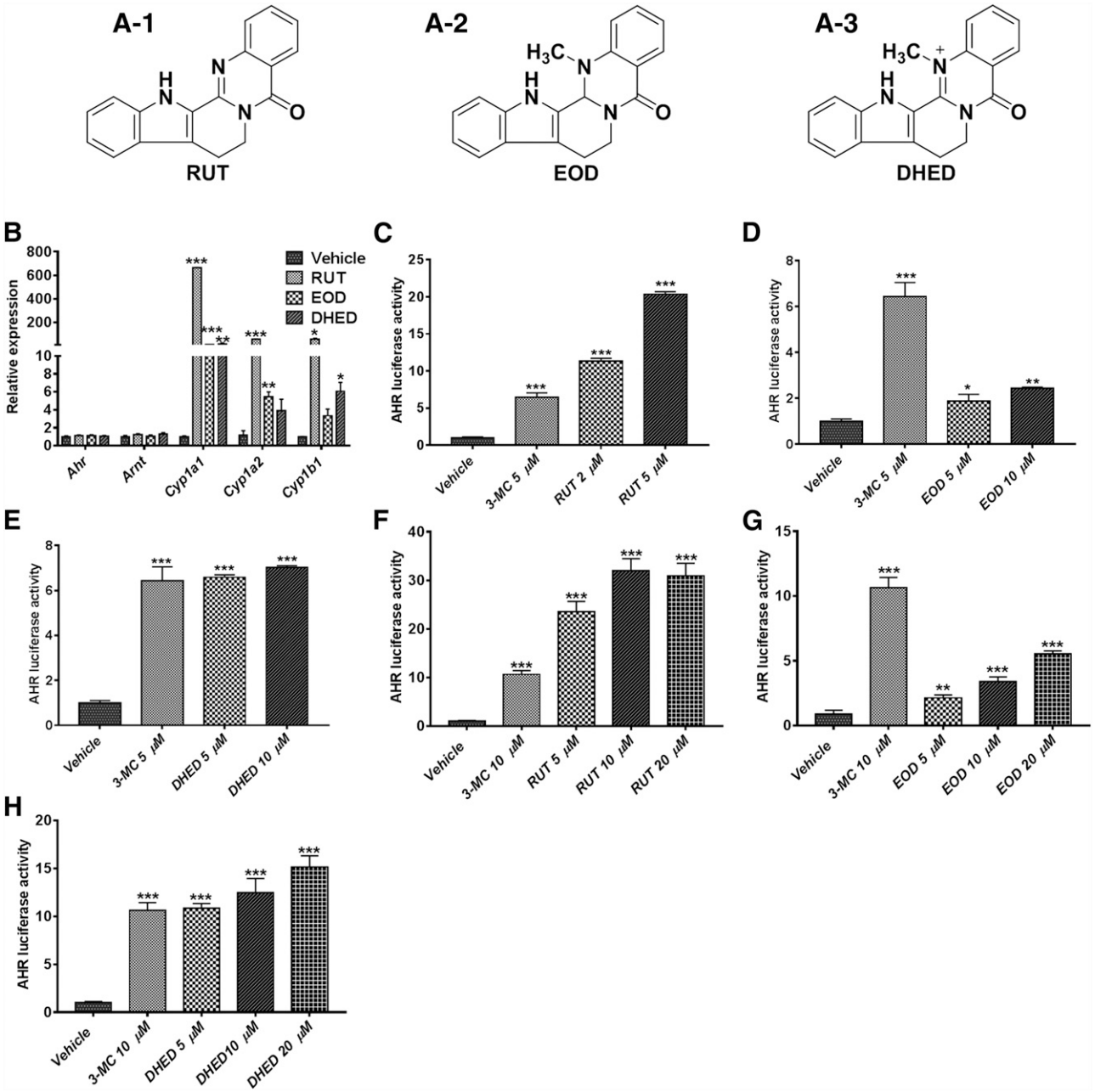

Fig. 1. Chemical structures and analysis of AHR target gene expression in primary hepatocytes by RUT, EOD, and DHED. (A1–A3) Chemical structures of RUT, EOD, and DHED. (B) qPCR analysis of mRNA expression for AHR target genes in mouse primary hepatocytes after treatment with the tested compounds RUT, EOD, and DHED at 5 μM. Significance was determined by one-way analysis of variance test (*$P < 0.05$; **$P < 0.01$; ***$P < 0.001$ vs. vehicle group). (C–H) Luciferase assays for AHR activation in HepG2 (C–E) and Hepa-1c1c7 cells (F–H). The values are presented as the mean ± S.E.M. *$P < 0.05$; **$P < 0.01$; ***$P < 0.001$, compared with that of AHR-luciferase + dimethylsulfoxide, by one-way analysis of variance test.

rutaecarpa. These three compounds showed a variety of intriguing biologic properties, such as antitumor, antithrombotic, anti-inflammatory, analgesic, antiobesity, anticholinesterase, and antiamnesic activities (Park et al., 1996; Sheu et al., 2000; Fei et al., 2003; Liao et al., 2005; Ko et al., 2007; Bak et al., 2010; Yu et al., 2013; Zhang et al., 2017), and RUT and EOD were specified as quantitative index components of *E. rutaecarpa* in the Chinese Pharmacopoeia (Committee of Chinese Pharmcopeia, 2015).

RUT, EOD, and DHED have the same basic skeleton as indoloquinazoline alkaloids, with different substituents only at the N-14 atom (Fig. 1A). Although no data exist on the role of DHED in AHR activation, RUT was demonstrated as an AHR agonist that significantly induced *CYP1A1* mRNA and CYP1A1 protein levels through an AHR-dependent mechanism in Hepa-1c1c7 and HepG2 cell lines (Han et al., 2009; Stejskalova et al., 2011), whereas EOD was shown to suppress 2,3,7,8-tetrachlorodibenzo-p-dioxin (TCDD)–induced AHR activation in human Lovo cells (Yu et al., 2010), suggesting that these three indoloquinazoline alkaloids could possibly affect AHR activation in different ways due to substituents at the N-14 atom.

AHR activation is known to cause hepatotoxicity (Fader and Zacharewski, 2017), hepatic steatosis (Kawano et al., 2010), systemic metabolic dysfunction (Zhang et al., 2015), and bile acid disruption

(Gao et al., 2016). "Shennong's Classic of Materia Medica," the most ancient herbal medicine book in China, has recorded *E. rutaecarpa* as producing mild toxicity in humans (Yang, 1998). Recently, some studies demonstrated that *E. rutaecarpa* administration leads to liver toxicity (Qi et al., 2011; Cohen et al., 2012), whereas others found no significant hepatotoxicity (Yang, 2008). Similarly, as the major constituents, RUT, EOD, and DHED were also reported to have potential hepatotoxicity (Zhang et al., 2011; Lin et al., 2015). Thus, whether *E. rutaecarpa* causes hepatotoxicity varies based on experimental conditions and remains controversial.

Metabolomics has been used to investigate changes in endogenous metabolites after administration of traditional Chinese medicines (Zhang et al., 2010a; Wang et al., 2017). Although one study revealed that *E. rutaecarpa* altered endogenous metabolites (Zhang et al., 2010b), the mechanism of these changes and their role in efficacy and toxicity remain unexplored. Notably, the role of RUT, EOD, and DHED in modulating the endogenous metabolome is also not known. In the present study, RUT, EOD, and DHED were examined for their effects on endogenous metabolites and to determine AHR structure-activity relationships. These compounds are all AHR ligands, and the methyl substitute at the N-14 atom in their structures determines AHR activation potency as well as AHR-mediated bile acid disruption. These findings could facilitate a more complete understanding of the structure-activity relationships in AHR activation among indoloquinazoline alkaloids isolated from *Euodia ruticarpa*, and could be of benefit to guide clinical application of these drugs and to possibly develop more potent and less toxic derivatives.

Materials and Methods

Chemicals and Reagents. RUT, EOD, and DHED were isolated with a purity >98%, and the structures were determined with NMR and high resolution mass spectrometry (Zhang et al., 1999; Yang and Tang, 2007). Corn oil and dimethylsulfoxide were supplied by Sigma Chemical Co. (St. Louis, MO). Fetal bovine serum (FBS), Dulbecco's modified Eagle's medium, and sodium pyruvate were obtained from Gibco-BRL (Grand Island, NY). Chlorpropamide was purchased from J&K Co. (Beijing, China). TRIzol reagent and Lipofectamine 3000 reagent were purchased from Thermo Fisher Scientific (Halethorpe, MD). TRIzol reagent and penicillin/streptomycin were obtained from Invitrogen (Carlsbad, CA). qScriptTM cDNA SuperMix was from Quantabio (Beverly, MA).

Culture of Primary Hepatocytes. Primary hepatocytes were isolated from C57BL/6N mice (6–8 weeks) and seeded on 12-well plates (2×10^4/well) as previously reported (Seglen, 1976). After starvation with FBS-free Williams' medium E for 2 hours, the hepatocytes were exposed to different concentrations of RUT, EOD, DHED, or 10 μM of 3-methylcholanthrene (3-MC; positive control) for 24 hours. After washing twice with phosphate-buffered saline, the hepatocytes were collected and lysed for gene-expression analysis.

Real-Time Polymerase Chain Reaction. Total RNA of each well was extracted with 1 ml of TRIzol (Takara, Japan) reagent. cDNA was then reverse transcribed from the RNA using qScriptTM cDNA SuperMix. The products were diluted to 1:10 using diethylpyrocarbonate-treated water. Quantitative polymerase chain reaction (qPCR) analysis was performed on an ABI 7500 real-time PCR and used SYBR Green Invitrogen (Carlsbad, CA) probe to conduct the real-time PCR. Sequences of qPCR primers used in this study are shown in Supplemental Table 1. The reaction values were calculated utilizing the $^{\Delta\Delta}$CT method. The mRNA levels were normalized to corresponding *Actb* mRNA.

Culture of Cell Lines and Luciferase Assays. HepG2 and Hepa-1c1c7 cells, obtained from the American Type Culture Collection (Manassas, VA), were cultured in a humidified atmosphere in 5% CO_2 at 37°C in Dulbecco's modified Eagle's medium complemented with nonessential amino acids, 10% FBS, and 1% penicillin/streptomycin. For the luciferase assays, pCMV6-XL4-AHR (human; OriGene Technologies, Rockville, MD), pcDNA3/βAHR (mouse), pGudLuc 6.1 plasmids [dioxin-responsive element (DRE)–driven luciferase reporter, kindly provided by Gary H. Perdew, Penn State University, State College, PA], and pCMV-renilla luciferase vector (kindly provided by Grace L. Guo, Rutgers University, New Brunswick, NJ) were used. Cells were seeded into 24-well plates (1×10^5 cells/well). The plasmids were transfected using Lipofectamine 3000 reagent (Thermo Fisher Scientific). The DRE-driven luciferase reporter was cotransfected with human or mouse AHR expression plasmid into HepG2 cells or Hepa-1c1c7 cells, respectively. In the control wells, pCMV6 empty vector was transfected. Twenty-four hours after transfection, the cells were treated with various concentrations of RUT, EOD, DHED, or the positive control 3-MC. Twelve hours after treatment with drugs, luciferase activities were quantified using a Dual Luciferase Kit from Promega (Madison, WI) with a Veritas Microplate Luminometer plate reader from Tuner Biosystems (Sunnyvale, CA). Transfection efficiency was normalized by renilla luciferase activity.

Molecular Docking. To investigate the details of the interaction of AHR with the compounds, the small soluble promiscuous ligand-binding C-terminal PAS domain of the human AHR (AHR-PAS-B) was selected (Fukunaga et al., 1995; Beischlag et al., 2008). Molecular docking was run into the homology model of the human AHR-PAS-B as previously described with TCDD as a positive control (Perkins et al., 2014).

Animal Studies. Male C57BL/6N (6–8 weeks old) mice were obtained from the National Institutes of Health contractor (Charles River Laboratories, Inc., Frederick, MD). All experimental procedures were in compliance with the animal study protocols approved by the National Cancer Institute Animal Care and Use Committee and the guidelines for the use of experimental animals of the Peking University Committee on Animal Care and Use (SYXK[Jing]2006-0025). The mice were housed in a specific pathogen-free environment controlled for temperature and light (25°C, 12-hour light/dark cycle) and humidity (45%–65%). The experiments were started after acclimatization for 1 week in the National Cancer Institute vivarium. Age-matched male, 6–8-week-old $Ahr^{+/+}$ and $Ahr^{-/-}$ mice were described previously (Gao et al., 2016). For the time-course study, wild-type C57BL/6N mice were randomly divided into 12 groups with five mice per group, and then treated with RUT, EOD, or DHED (80 mg/kg, suspended in 0.5% carboxymethyl cellulose sodium) or with vehicle (0.5% carboxymethyl cellulose sodium) by gavage once a day for 3, 12, and 21 days. For long-term toxicity studies, age-matched male $Ahr^{+/+}$ and $Ahr^{-/-}$ mice were randomly divided into four groups and treated with vehicle or RUT, EOD, or DHED at 80 mg/kg for 21 days. At the prescribed time points, the mice were killed after 4-hour fasting, and blood was collected immediately following CO_2 asphyxiation and centrifuged for 10 minutes at 8000*g* at 4°C to collect serum, which was immediately frozen and kept at −80°C until analysis. Liver samples were collected for histopathological analysis. For pharmacokinetic studies, each experimental group had 15 male C57BL/6N mice, and the mice were divided into three subgroups. After oral administration of the compounds, blood was collected at 0.08, 0.5, 1, 2, 4, 6, 8, 12, and 24 hours (each subgroup was collected three times).

Histopathology Assessment. Small blocks of mouse liver tissues were fixed with 10% neutral formalin and embedded in paraffin. After being stained with H&E, the slides were observed under a pathologic microscope. Alanine aminotransferase (ALT) and aspartate aminotransferase (AST) kits (Catachem Inc., Oxford, CT) were used to test serum ALT and AST levels.

Liquid Chromatography–Tandem Mass Spectrometry Analysis. The liquid chromatography–tandem mass spectrometry (MS/MS) system [ultra-performance liquid chromatography (UPLC)–MS/MS-8050 system; Shimadzu Corporation, Kyoto, Japan] contains a Shimadzu 30 CE liquid chromatography system (an SIL-30AC autosampler, an LC-30A binary pump, an SPD-M30A PDA detector, and a CTO-20AC column oven) and an 8050 triple quadrupole mass spectrometer consisting of a heated electrospray ionization source. Data acquisition was operated by the LabSolutions LCMS Version 5.6 software (Shimadzu, Columbia, MD). Multiple reaction monitoring mode was used for quantitation of the transitions of m/z 288.1→273.1 for RUT, 304.1→134.1 for EOD, 302.1→286.1 for DHED, and 237.1→194.1 for internal standard. Analysis details for sample processing, preparation of standards, and experiment conditions for liquid chromatography–MS/MS analysis are listed in the Supplemental Methods.

Calculation of Pharmacokinetic Parameters and Physicochemical Prediction In Silico. Pharmacokinetic parameters were calculated with Das 2.0 software (Drug and Statistics 2.0; Mathematical Pharmacology Professional Committee of China, Shanghai, China), a widely used software for pharmacokinetic parameter calculation (Yang et al., 2017). In addition, physicochemical

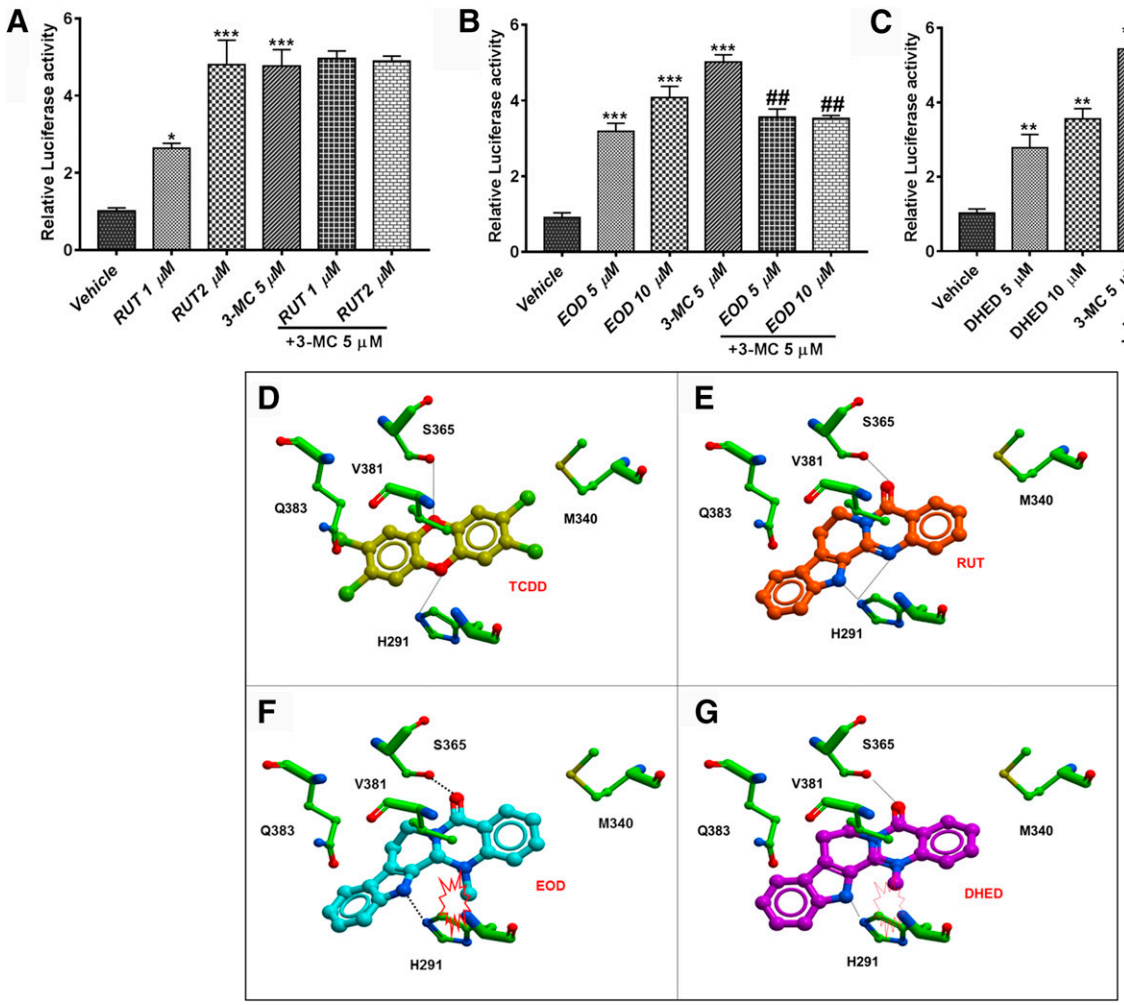

Fig. 2. Structure-activity relationship analysis of the tested compounds on AHR activation. (A–C) Luciferase assays for AHR activation in HepG2 after treatment with the tested compounds in the presence or absence of 3-MC. (D–G) Docking pose of TCDD, RUT, EOD, and DHED in the human AHR-PAS-B binding pocket; the ligands are displayed as sticks and colored by atom type, with carbon atoms in yellow (TCDD), orange (RUT), cyan (EOD), and magenta (DHED); residues are displayed as sticks and colored by atom type with carbon atoms in green. Data are presented as the mean ± S.E.M. (n = 3). $^{*}P < 0.05$; $^{**}P < 0.01$; $^{***}P < 0.001$ vs. vehicle group; $^{\#}P < 0.05$; $^{\#\#}P < 0.01$ vs. 3-MC group, by one-way analysis of variance test.

prediction in silico was performed with the ACD/Percepta Platform available online (Advanced Chemistry Development, Inc., Toronto, Canada). For the analysis, the ACD/Percepta Platform software was loaded with the structure of the compounds generated in the ".mol" format. The predictions were obtained based on quantitative structure-activity relationship models, and some physicochemical parameters associated with bioavailability were calculated as described previously (Avdeef, 2001; Shang et al., 2014).

UPLC-MS/MS Analysis and Multivariate Data Analysis. Metabolomic analysis was performed on an ultra-performance liquid chromatography coupled Xevo G2 quadrupole time-of-flight mass spectrometer with an ACQUITY UPLC (Waters, Milford, MA) as previously described (Jiang et al., 2015). Analytes of cholic acid (CA), α-muricholic acid (α-MCA), β-muricholic acid (β-MCA), ω-muricholic acid (ω-MCA), deoxycholic acid, lithocholic acid, taurocholic acid, tauro (T)-α-MCA, T-β-MCA, T-γ-MCA, T-ω-MCA, taurodeoxycholic acid (T-DCA), taurochenodeoxycholic acid, tauroursodeoxycholic acid, taurohyodeoxycholic acid, and taurolithocholic acid in gallbladder extracts were quantified with taurocholic acid-d5 as the internal standard. Individual standard curves established as $\text{area}_{\text{analyte}}/\text{area}_{\text{internal}}$ were used to calculate the concentrations of bile acids in samples.

Statistical Analysis. Statistical analysis was performed on Prism version 7.0 by using one-way analysis of variance followed by Dunnett's multiple comparisons test among multiple-group comparisons (GraphPad Software, San Diego, CA). The values are presented as the mean ± S.E.M. with $P < 0.05$ considered statistically significant as stated. Principal components analysis (PCA) and orthogonal partial least-squares discriminant analysis were performed on SIMCA-P software 13.0 (Umetrics, Umea, Sweden).

Results

RUT, EOD, and DHED Regulate AHR Battery Gene Expression in Mouse Primary Hepatocytes. To investigate whether RUT, EOD, and DHED could directly activate the AHR, hepatocytes were treated with 5 μM of these three compounds, respectively. In addition, AHR target gene mRNAs, including *Cyp11*, *Cyp12*, and *Cyp1b1*, were all significantly upregulated, among which *Cyp1a1* mRNA was markedly induced by 665-, 12.5-, and 20.6-fold by RUT, EOD, and DHED, with an efficacy order of RUT > DHED > EOD (Fig. 1B). These data demonstrate that RUT, EOD, and DHED could activate AHR and suggest that RUT has the strongest activity toward AHR activation among the three compounds.

RUT, EOD, and DHED Activate AHR in Luciferase Reporter Gene Assays in HepG2 and Hepa-1c1c7 Cell Lines. To confirm whether RUT, EOD, and DHED activate the AHR, luciferase reporter gene assays were performed with DRE-driven luciferase reporter and

TABLE 1
ICM scores of TCDD, RUT, EOD and DHED into human AHR-PAS-B

Compound	HID	HIE
TCDD	−24	−26
RUT	−8.99	−14.5
EOD	nd	nd
DHED	nd	nd

HID, H291-D; HIE, H291-E; nd, not docked favorably (positive scores).

human AHR expression plasmids (Gao et al., 2016). With 3-MC as a positive control, RUT, EOD, and DHED dose-dependently activated AHR in HepG2 (Fig. 1, C–E) and Hepa-1c1c7 cells (Fig. 1, F–H). At 5 μM, RUT, EOD, and DHED induced luciferase activity by 20.4-, 2.43-, and 6.60-fold, respectively, in HepG2 cells, and 23.6-, 2.14-, and 10.8-fold, respectively, in Hepa-1c1c7 cells. Consistent with the primary hepatocyte data, these results suggest that RUT has the strongest activity among the three compounds, and confirm that RUT, EOD, and DHED activate the AHR with an efficacy order of RUT > DHED > EOD.

To further test how these compounds could affect 3-MC–induced AHR activation, HepG2 cells were treated with different concentrations of RUT, EOD, and DHED in the presence or absence of 3-MC. Whereas RUT treatment alone was found to efficiently induce AHR activation at both 1 and 2 μM, combined treatment of RUT with 5 μM 3-MC showed a responses comparable with 3-MC treatment alone (Fig. 2A). In contrast, 3-MC–induced AHR activation was significantly suppressed by both EOD and DHED at 5 and 10 μM (Fig. 2, B and C). These results suggest that RUT, the most potent AHR activator among the three compounds, did not significantly affect 3-MC–induced AHR activation at the concentrations used, whereas EOD and DHED, as potentially relatively weak AHR agonists compared with 3-MC, could antagonize 3-MC–induced activation of AHR.

Ligand Docking of RUT, EOD, and DHED to the AHR. To explain how the AHR-activating effects vary among the three compounds, in silico molecular modeling and docking of RUT, EOD, and DHED to the AHR were performed. As a positive control, the potent full-agonist TCDD docked into the human AHR-PAS-B binding pocket with an average score of −25 in the presence of both tautomerization states of His291 (Table 1). As previously reported, TCDD establishes a dual hydrogen-bonding (HB) interaction with the side chain of Ser365 and His291 (Fig. 2D) (Perkins et al., 2014). The three alkaloids RUT, EOD, and DHED were docked into the human model. Compared with TCDD, RUT docked with a lower but favorable score in both tautomerization states of His291 (Table 1). The binding manner of RUT, EOD, and DHED revealed the dual HB pattern, which was also observed with the positive control TCDD (Fig. 2, E–G). However, poor scores were obtained with EOD and DHED, indicating that the methyl group at nitrogen (N-14) of the quinazolin-5(7H)-one ring could be a determining factor for binding (Fig. 2, F and G; Table 1). Further analysis of three-dimensional conformation confirmed that the change of the pyrido[2,1-b]-quinazolin-5(7H)-one system could lead to an energetically unfavorable steric clash between the 14-methyl group of EOD and DHED and the imidazole ring of His291 (data not shown).

RUT, EOD, and DHED Induction of CYP1 Family mRNA Expression In Vivo Is AHR-Dependent. To further determine whether RUT, EOD, and DHED possess activity toward AHR in vivo, mice were treated daily by intragastric gavage at 80 mg/kg for 3, 12, and 21 days, respectively, and the time-course expression of *Cyp1a1*, *Cyp1a2*, and *Cyp1b1* mRNAs in livers was measured. Consistent with the in vitro results, the mRNA expression of *Cyp1a1*, *Cyp1a2*, and *Cyp1b1* in the RUT- and DHED-treated groups was induced across the duration of drug administration, whereas no induction was noted in the EOD-treated group (Fig. 3). To further determine whether the effects of these alkaloids on CYP1 family mRNAs is dependent on AHR, RUT, EOD, and DHED were administered to age-matched $Ahr^{+/+}$ and $Ahr^{-/-}$ mice for 21 days. The mRNA levels of AHR target genes were induced by RUT and DHED in the livers of $Ahr^{+/+}$ mice, but not in the $Ahr^{-/-}$ mice (Fig. 4, A and B). These results confirmed that RUT and DHED could significantly induce AHR-dependent mRNA induction of CYP1 family genes. Notably, although DHED is a relatively weaker AHR activator in vitro compared with RUT, a comparable mRNA induction of AHR target genes by DHED and RUT was found in vivo (Fig. 4, A and B). In contrast to the AHR-activating effect of EOD in vitro, no significant change of AHR target gene expression was noted in vivo by EOD administration to mice for 3, 12, and 21 days, as well as 21-day treatment of $Ahr^{+/+}$ and $Ahr^{-/-}$ mice. These data demonstrated that RUT and DHED induced AHR-dependent induction of the CYP1 family in vivo, whereas EOD failed to activate AHR in vivo in contrast to in vitro, suggesting that RUT, DHED, and EOD showed a differential effect in vivo compared with in vitro.

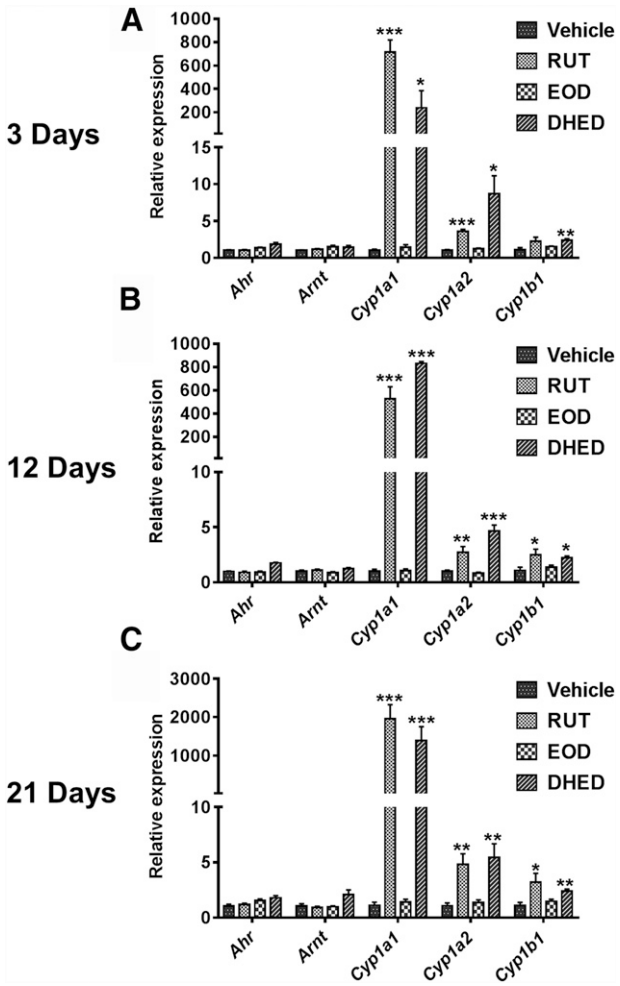

Fig. 3. Time-course study in wild-type mice after treatment with RUT, EOD, or DHED (80 mg/kg, gavage). (A) AHR and its target battery gene mRNA expression after 3 days of treatment. (B) AHR and its target gene mRNA expression after 12 days of treatment. (C) AHR and battery gene expression after 21 days of treatment. Data are presented as the mean ± S.E.M. (n = 5/group). The values are presented as mean ± S.E.M. *$P < 0.05$; **$P < 0.01$; ***$P < 0.001$ vs. vehicle group, by one-way analysis of variance test.

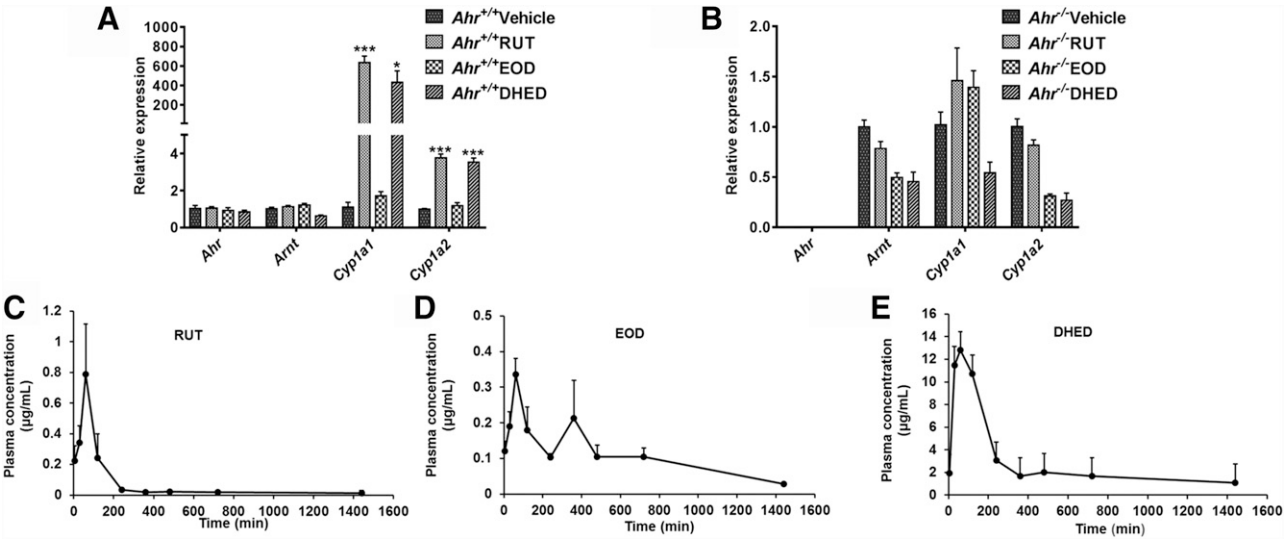

Fig. 4. In vivo AHR-activating effects and pharmacokinetic behaviors of RUT, EOD, or DHED after treatment (80 mg/kg, gavage) for 21 days in both $Ahr^{+/+}$ and $Ahr^{-/-}$ mice. (A) AHR and its target battery gene expression after 21-day treatment in $Ahr^{+/+}$ mice. (B) AHR and its target battery gene expression after 21-day treatment in $Ahr^{-/-}$ mice. (C–E) Time course of plasma concentration for RUT, EOD, and DHED after treatment (80 mg/kg, gavage). Data are presented as the mean ± S.E.M. (n = 5/group). $^{*}P < 0.05$; $^{***}P < 0.001$ vs. vehicle group, by one-way analysis of variance test.

Physicochemical Properties and Pharmacokinetics of the Alkaloids. Given that the extent of AHR activation in vivo by RUT, DHED, and EOD is not totally consistent with the results in vitro, the different oral absorption in mice was further predicted to account for this discrepancy. To test this hypothesis, physicochemical prediction in silico and pharmacokinetic studies were performed. DHED showed the maximum intrinsic solubility (0.14 mg/ml) among the three compounds (Table 2). Solubility in the intestinal tract is an important factor affecting absorption of compounds (Dressman et al., 2007). The in silico analysis of physicochemical prediction showed that intrinsic solubility of DHED was 0.14 mg/ml, whereas RUT and EOD were 0.02 and 0.01 mg/ml, respectively (Table 2). These data indicate DHED has a maximum value of intrinsic solubility and may explain why the effect of DHED on AHR activation is abnormally high in vivo compared with its relatively weaker in vitro AHR-activating effect. To further confirm this view, pharmacokinetic studies of the three compounds were carried out after intragastric gavage to mice at a dose of 80 mg/kg, respectively (Fig. 4, A, B and C). The pharmacokinetic parameter calculation showed the C_{max} by DHED treatment ranked highest with a value of 12.8 ± 2.39 μg/ml, much higher than 0.80 ± 0.54 μg/ml by RUT and 0.34 ± 0.22 μg/ml by EOD (Fig. 4, C–E; Table 2). Similarly, DHED treatment showed the highest AUC value. These data demonstrate that DHED has a greater degree of exposure in vivo, whereas EOD has the lowest C_{max} value. Therefore, the better absorption of DHED could be at least one factor that facilitates its activation of AHR in vivo, and the relatively poor absorption of RUT and EOD could compromise their AHR-activating effect in vivo.

RUT, EOD, and DHED Are Not Hepatotoxic. The potential for liver toxicity induced by RUT, EOD, and DHED was then investigated. Liver and serum of mice treated with the three compounds by daily intragastric gavage for 3, 12, and 21 days in C57BL/6N mice were analyzed. Mice treated with the three compounds during the time course exhibited no significant differences in liver/body weight ratios, which suggests that these three compounds caused no significant hepatomegaly (Fig. 5, A–C). Moreover, no obvious differences in serum ALT and AST activities were found between vehicle and drug-treatment groups (Fig. 5, D–I), indicating no obvious liver toxicity. In agreement, treatment with RUT, EOD, and DHED for 21 days in both $Ahr^{+/+}$ and $Ahr^{-/-}$ mice was further confirmed to show no significant hepatotoxicity by histology analysis, liver/body weight ratios, and serum biochemistry analysis (Fig. 6). These data consistently demonstrated that these three compounds are not hepatotoxic in mice under the experimental conditions used.

TABLE 2

Physicochemical property and pharmacokinetic parameters

Values are the mean ± S.E.M.

Parameters	RUT	EOD	DHED
LogP	2.40	2.34	−2.30
pKa	3.43	4.29	—
Pe (cm/s) (pH = 7.4)	2.10×10^{-4}	2.06×10^{-4}	2.00×10^{-7}
Intrinsic solubility (mg/ml) (pH = 7.4)	0.02	0.01	0.14
TPSA (Å^2)	48.5	39.3	39.1
$T_{1/2}$ (minutes)	56.4 ± 4.23	69.3 ± 0.1	64.0 ± 3.45
T_{max} (minutes)	54.0 ± 3.66	66.0 ± 5.74	60.0 ± 0.1
C_{max} (μg/ml)	0.80 ± 0.54***	0.34 ± 0.22###	12.8 ± 2.39
$AUC_{0\sim t}$ (μg/ml ·min)	80.2 ± 4.89***	151 ± 5.78###	3450 ± 34.6
$AUC_{0\sim\infty}$ (μg/ml ·min)	83.4 ± 4.64***	186 ± 6.02###	4760 ± 36.1

Pe, permeability; TPSA, topological polar surface area.
$^{***}P < 0.001$, RUT group vs. DHED group; $^{\#\#\#}P < 0.001$, EOD group vs. DHED group.

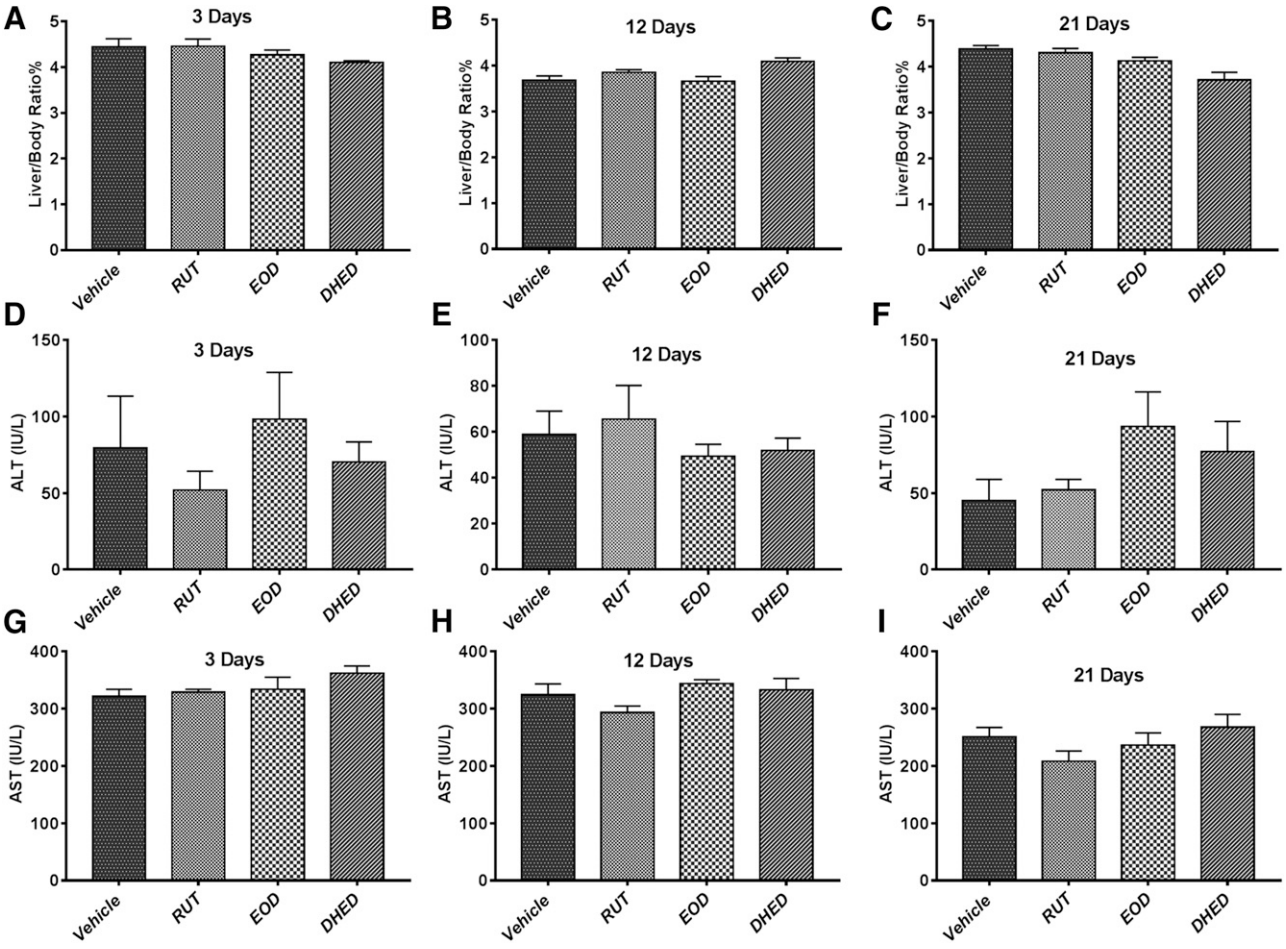

Fig. 5. Time course of the hepatotoxicity response in C57BL/6N mice after treatment with vehicle (0.5% carboxymethyl cellulose sodium) and RUT, EOD, and DHED, respectively (80 mg/kg, gavage). (A–C) Changes in liver weight/body weight ratios. (D–F) Changes in ALT in serum. (G–I) Changes in AST in serum. Data are presented as the mean ± S.E.M. (n = 5 mice/group). One-way analysis of variance was used for statistical analysis.

RUT and DHED Treatment Impairs Bile Acid Homeostasis. Although the tested compounds did not cause significant hepatotoxicity, it is still possible that they could cause a disturbance in endogenous metabolism via AHR activation. Since hepatic AHR activation in vivo was only found with RUT and DHED but not with EOD, samples from mice treated with RUT and DHED were chosen for further global metabolomic analysis. First, RUT-treated $Ahr^{+/+}$ mice showed a significantly darkened gallbladder, which was not observed in $Ahr^{-/-}$ mice (data not shown). Thus, global metabolomics was performed with bile to profile the metabolites in gallbladder from treated mice. Metabolites derived from RUT and DHED were excluded from the multivariate data analysis to ensure the distinction was not caused by exogenous metabolites from RUT and DHED. PCA was used to analyze both vehicle- and drug-treated groups. PCA modeling showed a significant separation in mice treated with RUT and DHED in $Ahr^{+/+}$ mice (Fig. 7, A and B), but not in the $Ahr^{-/-}$ mice (Fig. 7, C and D). Then, orthogonal partial least-squares discriminant analysis was performed to produce loading scatter S-plots (Fig. 8, A and B). The ions that contributing to separation caused by RUT and DHED treatment were selected according to the abundance ranks and correlations after primary screening, among which several potential bile acid metabolites were listed. The identity of the bile acid metabolites and their quantification were determined with UPLC-MS/MS by use of authentic standards (Yu et al., 2010). Compared with the vehicle-treated group, levels of unconjugated bile acids (CA, α-MCA, β-MCA, ω-MCA, and deoxycholic acid) were found to be significantly increased in RUT-treated $Ahr^{+/+}$ mice (Fig. 8C). Similarly, unconjugated bile acids, CA and ω-MCA, were significantly upregulated, while α-MCA and β-MCA tended to be slightly increased, by DHED treatment (Fig. 8C). For taurine-conjugated bile acids, RUT treatment was found to significantly increase the levels of taurocholic acid, T-DCA, tauroursodeoxycholic acid, and taurohyodeoxycholic acid, whereas DHED was found to significantly increase the levels of taurocholic acid and T-DCA (Fig. 8D). As expected, no change in bile acid concentrations was observed in $Ahr^{-/-}$ mice after treatment with either RUT or DHED for 21 days (Fig. 8, E and F). These findings further demonstrate that RUT and EOD disrupt bile acid homeostasis through an AHR-dependent mechanism.

To explain how RUT and DHED could disturb bile acid homeostasis in vivo, expression of mRNAs associated with bile acid synthesis and transport was analyzed. Consistent with the bile acid disruption data, *Cyp7a1* mRNA encoding the rate-limiting enzyme for bile acid synthesis was significantly induced by RUT treatment in $Ahr^{+/+}$ mice but not in $Ahr^{-/-}$ mice, whereas the mRNA encoding the bile salt export pump (BSEP) was increased in DHED-treated $Ahr^{+/+}$ mice, but not in $Ahr^{-/-}$ mice (Fig. 8, G and H). These observations indicate that the compounds disrupt bile acid homeostasis dependent on AHR, although the exact mechanism of how RUT and DHED regulate the induction of CYP7A1 or BSEP via AHR activation still requires further investigation.

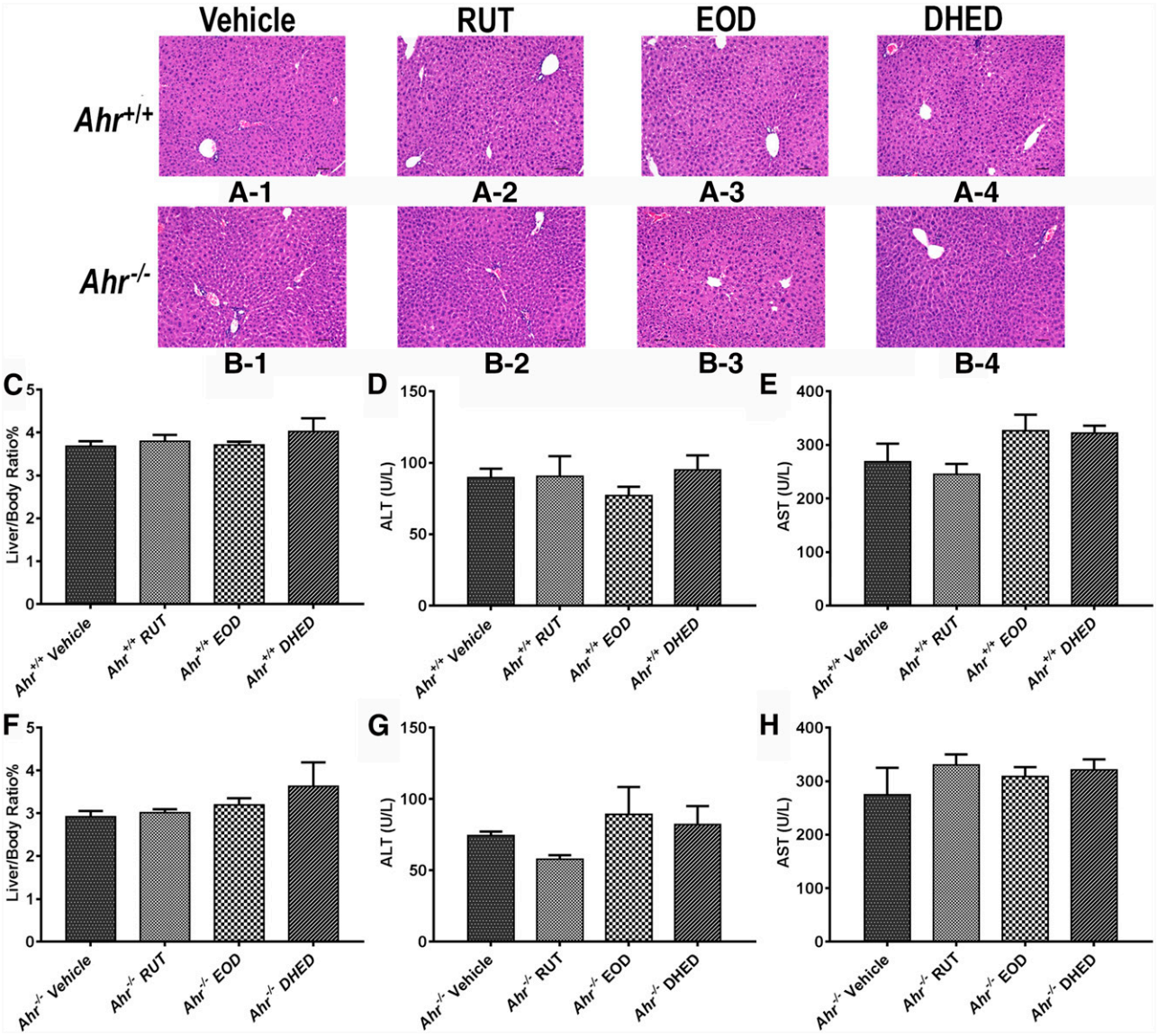

Fig. 6. The hepatotoxicity response in $Ahr^{+/+}$ mice and $Ahr^{-/-}$ mice after treatment with control vehicle (0.5% carboxymethyl cellulose sodium), RUT, EOD, and DHED at a dose of 80 mg/kg, respectively. (A1–A4) Light microscopic examination of H&E-stained liver sections of $Ahr^{+/+}$ mice after 21-day treatment; scale bar, 50 μm; original magnification, 20×. (B1–B4) Light microscopic examination of H&E-stained liver sections of $Ahr^{-/-}$ mice after 21-day treatment; scale bar, 50 μm; original magnification, 20×. (C–E) Changes in liver weight/body weight ratios, serum ALT levels, and AST levels in $Ahr^{+/+}$ mice. (F–H) Changes in liver weight/body weight ratios, serum ALT levels, and AST levels in $Ahr^{-/-}$ mice. Data are presented as the mean ± S.E.M. (n = 5/group). One-way analysis of variance test was used for statistical analysis.

Discussion

In the current study, by taking advantage of the high structural similarity of the major components of *E. rutaecarpa*, RUT, EOD, and DHED, a methyl group at the N-14 atom was found to be a determinant factor in mediating AHR activation in vitro. Based on the current study, RUT and DHED could induce AHR activation as well as AHR-dependent bile acid disruption in vivo. The differing absorption of the three compounds in vivo may explain why AHR activation by the tested compounds differed between in vivo liver and cultured mouse hepatocytes.

RUT, EOD, and DHED belong to the indoloquinazoline alkaloid class of compounds and are structural analogs. Whereas RUT and EOD were found to affect AHR activation in previous studies (Han et al., 2009; Yu et al., 2010; Stejskalova et al., 2011), there is no report on the role of DHED in AHR activation. In the present study, RUT, EOD, and DHED could induce AHR target gene mRNAs in primary hepatocytes and DRE-driven luciferase reporter activity in HepG2 cells and Hepa-1c1c7 cells. Furthermore, luciferase assays revealed that EOD and DHED are weak agonists of AHR. Consistent with previous studies (Ueng et al., 2001; Han et al., 2009), the present work conclusively demonstrated that RUT is an efficacious AHR agonist. Although in contrast to an earlier report that EOD alone suppresses *CYP1A1* expression in human Lovo cells (Yu et al., 2010), EOD significantly induces CYP1A1 in hepatocytes as revealed in the current study. Similar to the previous finding that EOD could antagonize TCDD-induced AHR activation (Yu et al., 2010), the current work also demonstrates that EOD could antagonize 3-MC–induced AHR activation, which suggests that EOD and DHED are potentially weaker agonists or could produce steric hindrance that disturbs the binding of 3-MC at the AHR ligand-binding site, which is further supported by the computational predictions. First, RUT, EOD, and DHED dock, bind, and activate the AHR. The docking scores predict lower agonist potency of RUT when compared with TCDD and lower potency of EOD and DHED when compared with RUT, but also possibly predict competitive

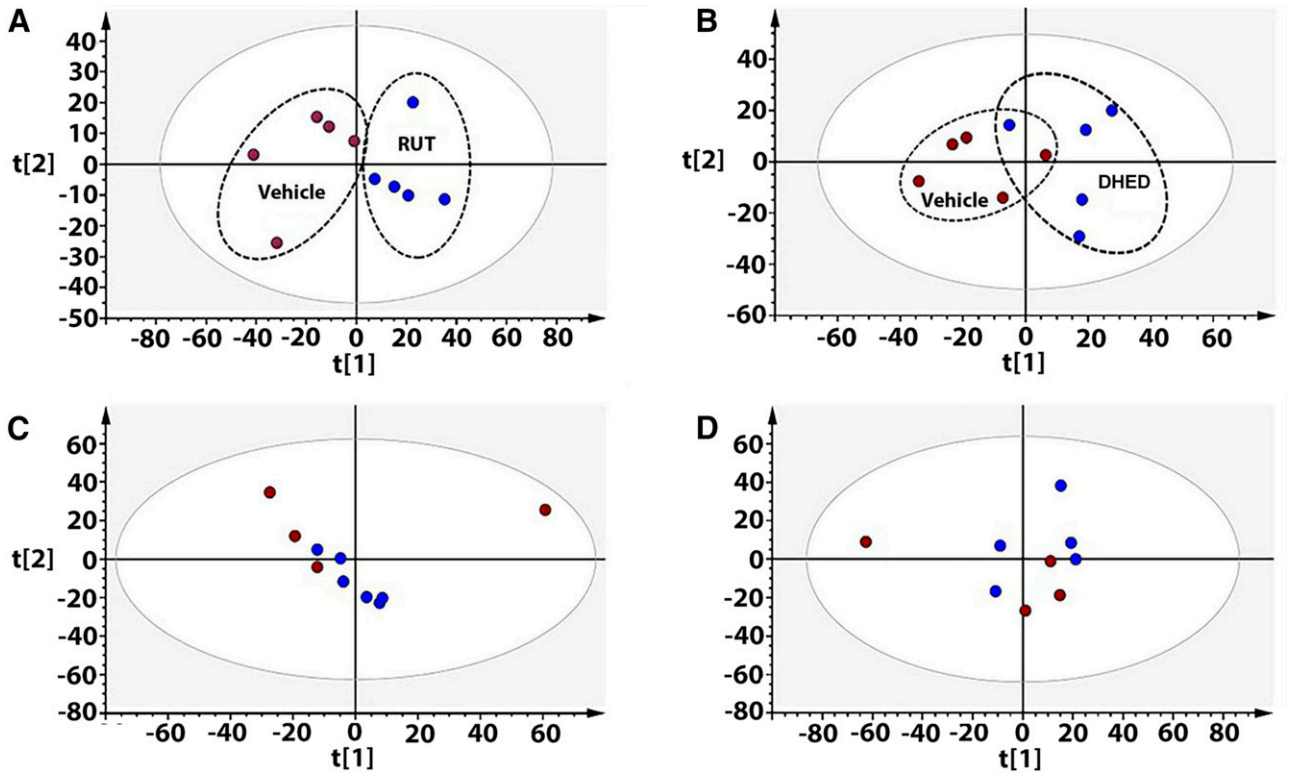

Fig. 7. PCA analysis of global metabolomes of bile acids; each point represents an individual mouse bile sample. (A and B) PCA analysis of global metabolomes in $Ahr^{+/+}$ mice treated with vehicle (0.5% carboxymethyl cellulose sodium) and RUT and DHED, respectively (80 mg/kg). (C and D) PCA analysis of global metabolomes in $Ahr^{-/-}$ mice treated with vehicle (0.5% carboxymethyl cellulose sodium) and RUT and DHED, respectively (80 mg/kg).

antagonism activity due to partial agonism. Since the structures of these three compounds only differ at N-14, the N-14 methyl group is likely to be a key factor that affects binding, and explains why EOD or DHED could antagonize 3-MC–induced activation as a result of steric hindrance. The poor scores obtained with EOD and DHED are probably due to the presence of the N-14 methyl group, which induces a three-dimensional conformation change in the pyrido[2,1-b]quinazolin-5(7H)-one system, leading to an energetically unfavorable steric clash between the 14-methyl group of EOD and DHED and the imidazole ring of His291. Additionally, the binding of RUT, EOD, and DHED in the human model revealed a dual HB pattern, which is also commonly observed with other known AHR agonists (Fukunaga et al., 1995; Perkins et al., 2014).

In the in vivo time-course study with RUT, DHED, and EOD, a high dose of 80 mg/kg was administered when compared with the doses used in previous studies that demonstrated toxicity of these compounds (Jeon et al., 2006; Zhang et al., 2011). In agreement with the in vitro studies, *Cyp1a1* and *Cyp1a2* mRNAs were markedly induced after RUT and DHED treatment in $Ahr^{+/+}$ mice but not in $Ahr^{-/-}$ mice, confirming that induction of the CYP1A family genes by both RUT and DHED is dependent on AHR. However, EOD failed to activate AHR battery genes in vivo across the time course, and DHED showed a relatively stronger effect of AHR activation compared with in vitro, almost equal to the effect of RUT in vivo. An intestinal transport study with Caco-2 cells found that uptake of RUT was lower than EOD and DHED (Yang et al., 2009). The uptake of these compounds occurs mainly via passive diffusion. Thus, there must be another reason for the difference in AHR activation between EOD and DHED. To explain this discrepancy, the physicochemical properties and pharmacokinetic behavior of the tested compounds were compared in vivo. Since solubility in the intestinal tract is an important factor affecting absorption of compounds (Dressman et al., 2007), in current study as shown in Table 2, the highest exposure of DHED in vivo is probably due to its high intrinsic solubility, which thus facilitates its AHR activation potential. In contrast, EOD demonstrates very low systemic exposure accompanied by low AHR activation potential in vivo, due to its relatively low intrinsic solubility. AHR activation by various ligands could induce a variety of physiologic and toxicological reactions (Fernandez-Salguero et al., 1996; Bunger et al., 2003; Gao et al., 2016). However, neither RUT and DHED, which strongly activated AHR, nor EOD, which did not activate AHR in vivo, caused any apparent hepatotoxicity or hepatomegaly in either $Ahr^{+/+}$ or $Ahr^{-/-}$ mice based on the integrated analysis of serum transaminases, liver histology, and liver index. In contrast to earlier studies (Zhang et al., 2011; Lin et al., 2015), RUT and EOD administration produced no hepatotoxicity when the tested compounds were administered at 80 mg/kg by gavage for up to 21 days in C57BL/6N mice. This is possibly due to different dosing methods, mouse background, or other experimental conditions. Although it is still possible that higher doses of RUT, EOD, and DHED administration for longer durations could cause liver toxicity, the failure to observe significant toxicity in the current experimental condition at least suggests that RUT, DHED, and EOD have a limited potential to cause hepatotoxicity.

To identify how the tested compounds could modulate endogenous metabolites via AHR activation, RUT and DHED, which were confirmed to activate AHR in vivo, were chosen for the study. Both RUT and DHED caused a significant increase of bile acid accumulation in the gallbladders of wild-type mice, although not in $Ahr^{-/-}$ mice, indicating an AHR-dependent effect. Consistent with its relatively higher activity for AHR activation in vitro, RUT was found to have a more significant effect on gallbladder appearance after treatment (data not shown), consistent with the marked accumulation of bile acid species (Fig. 8). Analysis of mRNAs involved in bile acid synthesis and transport reveals that RUT induces *Cyp7a1* mRNA, whereas DHED upregulates *Bsep* mRNA. In addition, no significant changes could be found with other bile

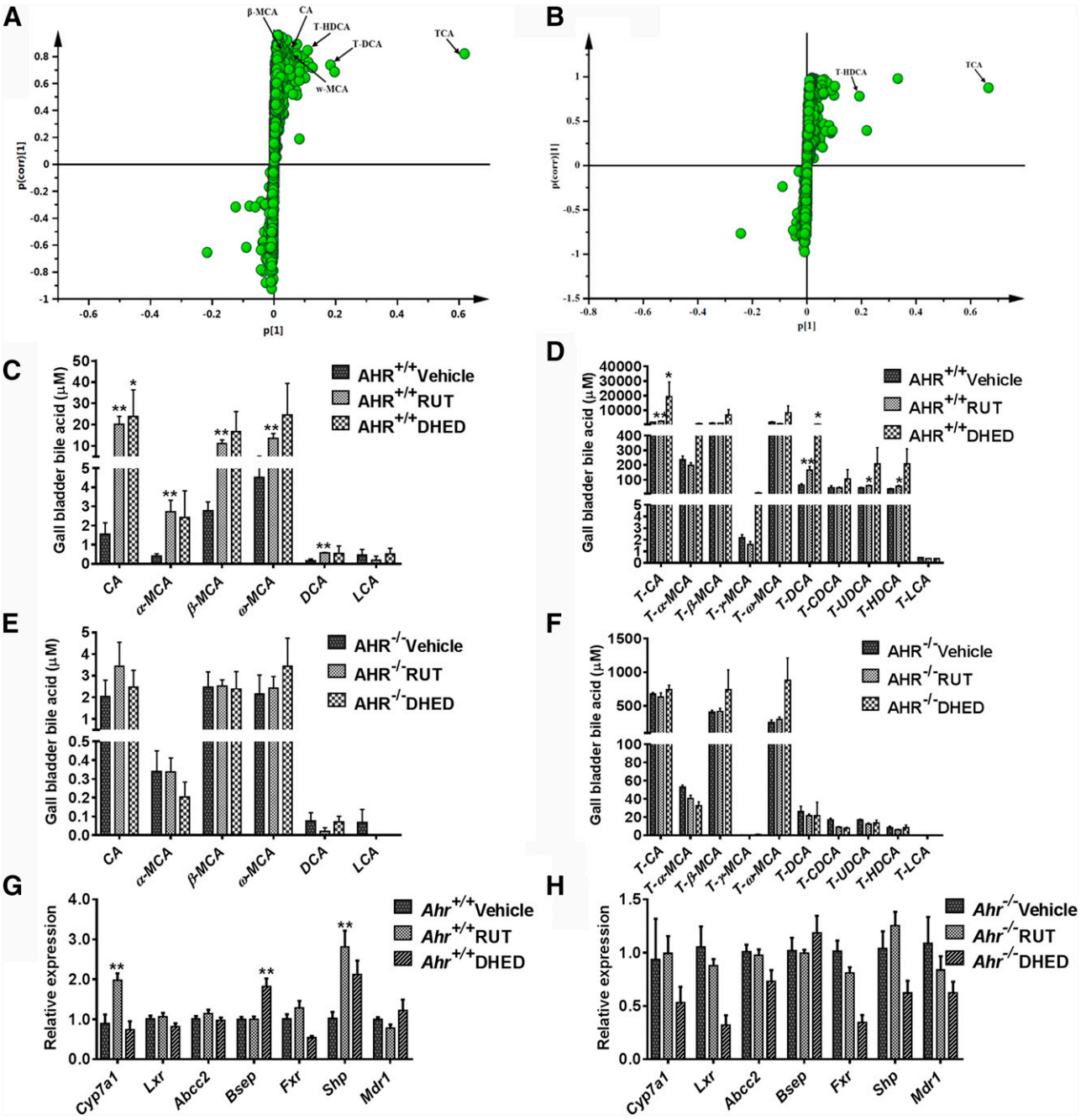

Fig. 8. Target quantitation of bile acid species and the bile acids signaling in $Ahr^{+/+}$ and $Ahr^{-/-}$ mice. $Ahr^{+/+}$ and $Ahr^{-/-}$ mice were treated with vehicle (0.5% carboxymethyl cellulose sodium) and RUT and DHED for 21 days, respectively (80 mg/kg). (A and B) S-plot of orthogonal partial least squares discriminant analysis of metabolome components in vehicle- and compound-treated $Ahr^{+/+}$ mice. (C and D) Target quantitation analysis of unconjugated bile acids (C) and conjugated bile acids (D) in bile of $Ahr^{+/+}$ mice. (E and F) Targeted quantitation analysis of unconjugated bile acids (E) and conjugated bile acids (F) in bile of $Ahr^{-/-}$ mice. (G and H) qPCR analysis of mRNA expression in the livers of $Ahr^{+/+}$ and $Ahr^{-/-}$ mice treated with RUT or DHED for 21 days. Data are presented as the mean ± S.E.M. (n = 5/group). *$P < 0.05$; **$P < 0.01$ vs. vehicle group, by one-way analysis of variance test. TCA, taurocholic acid; T-CDCA, taurochenodeoxycholic acid; T-HDCA, taurohyodeoxycholic acid; T-LCA, taurolithodeoxycholic acid; T-α-MCA, tauro-α-muricholic acid; T-β-MCA, tauro-β-muricholic acid; T-ω-MCA, tauro-ω-muricholic acid; T-UDCA, tauroursodeoxycholic acid.

acid transporters in liver (data not shown). Although RUT induced *Cyp7a1* mRNA in wild-type mice, *Fxr* (farnesoid X receptor) mRNA levels were not changed, and *Shp* (heterodimer partner; SHP inhibits *Cyp7a1* expression) mRNA levels were even enhanced, suggesting that *Cyp7a1* is upregulated by RUT independent of hepatic FXR-SHP signaling. Similarly, *Bsep* mRNA induction by DHED also does not occur through hepatic FXR signaling. On the other hand, intestinal FXR-FGF15 signaling was investigated and showed no difference after RUT and DHED treatments in the current study (data not shown), excluding the possibility that these compounds may influence intestinal FXR-FGF15 signaling, which is another pathway that regulates bile acid homeostasis. However, *Cyp7a1* and *Bsep* are not direct AHR target genes, and thus the exact mechanism by which RUT and DHED indirectly induce *Cyp7a1* and *Bsep* in vivo via AHR remains to be determined. Perhaps AHR-mediated activation of cytochrome P450 enzymes, including CYP1A1, CYP1A2, and CYP1B1, could directly

mediate the metabolism of endogenous compounds that modulate molecular signaling involved in bile acid synthesis and transport, and thus indirectly results in bile acid disruption.

In conclusion, by using the analogs, the current study highlights the substituent of the N-14 atom as a key determinant of AHR activation for indoloquinazoline alkaloids, RUT, DHED, and EOD, and demonstrates that RUT and DHED could activate AHR in vivo and cause AHR-dependent bile acid disruption without causing hepatotoxicity by upregulating *Cyp7a1* or *Bsep* through a mechanism that is yet to be determined. EOD fails to activate AHR in vivo, in contrast to its activating effect in vitro, due to its poor absorption in mice. These findings will be of benefit for a more complete understanding of the structure-activity relationships of indoloquinazoline alkaloids in activating AHR as well as informing on the potential for efficacy and toxicity in the clinical use of *E. ruticarpa*.

Acknowledgments

We thank Linda G. Byrd for assistance with the animal protocols and mouse studies.

Authorship Contributions

Participated in research design: Yo. Zhang, Yan, Gonzalez, Yang.

Conducted experiments: Yo. Zhang, Yan, Sun, Yi. Zheng, L. Zhang, Yagai.

Performed data analysis: Yo. Zhang, Yan, Xie, Krausz, Bisson.

Wrote or contributed to the writing of the manuscript: Yo. Zhang, Yan, Yang, Gonzalez.

References

Abel J and Haarmann-Stemmann T (2010) An introduction to the molecular basics of aryl hydrocarbon receptor biology. *Biol Chem* **391**:1235–1248.

Avdeef A (2001) Physicochemical profiling (solubility, permeability and charge state). *Curr Top Med Chem* **1**:277–351.

Bak EJ, Park HG, Kim JM, Kim JM, Yoo YJ, and Cha JH (2010) Inhibitory effect of evodiamine alone and in combination with rosiglitazone on in vitro adipocyte differentiation and in vivo obesity related to diabetes. *Int J Obes* **34**:250–260.

Bunger MK, Moran SM, Glover E, Thomae TL, Lahvis GP, Lin BC, and Bradfield CA (2003) Resistance to 2,3,7,8-tetrachlorodibenzo-p-dioxin toxicity and abnormal liver development in mice carrying a mutation in the nuclear localization sequence of the aryl hydrocarbon receptor. *J Biol Chem* **278**:17767–17774.

Cohen SM, Heywood E, Pillai A, and Ahn J (2012) Hepatotoxicity associated with the use of white flood, a nutritional supplement. *Pract Gastroenterol* **36**:45–47.

Committee of Chinese Pharmcopeia (2015) *Chinese Pharmacopeia*, pp 171–172, China Medical Science Press, Beijing, China.

Connor KT, Harris MA, Edwards MR, Budinsky RA, Clark GC, Chu AC, Finley BL, and Rowlands JC (2008) AH receptor agonist activity in human blood measured with a cell-based bioassay: evidence for naturally occurring AH receptor ligands in vivo. *J Expo Sci Environ Epidemiol* **18**:369–380.

Denison MS and Heath-Pagliuso S (1998) The Ah receptor: a regulator of the biochemical and toxicological actions of structurally diverse chemicals. *Bull Environ Contam Toxicol* **61**:557–568.

de Waard PW, Peijnenburg AA, Baykus H, Aarts JM, Hoogenboom RL, van Schooten FJ, and de Kok TM (2008) A human intervention study with foods containing natural Ah-receptor agonists does not significantly show AhR-mediated effects as measured in blood cells and urine. *Chem Biol Interact* **176**:19–29.

Dressman JB, Vertzoni M, Goumas K, and Reppas C (2007) Estimating drug solubility in the gastrointestinal tract. *Adv Drug Deliv Rev* **59**:591–602.

Fader KA and Zacharewski TR (2017) Beyond the aryl hydrocarbon receptor: pathway interactions in the hepatotoxicity of 2,3,7,8-tetrachlorodibenzo-*p*-dioxin and related compounds. *Curr Opin Toxicol* **2**:36–41.

Fei XF, Wang BX, Li TJ, Tashiro S, Minami M, Xing DJ, and Ikejima T (2003) Evodiamine, a constituent of Evodiae fructus, induces anti-proliferating effects in tumor cells. *Cancer Sci* **94**:92–98.

Fernandez-Salguero PM, Hilbert DM, Rudikoff S, Ward JM, and Gonzalez FJ (1996) Aryl-hydrocarbon receptor-deficient mice are resistant to 2,3,7,8-tetrachlorodibenzo-p-dioxin-induced toxicity. *Toxicol Appl Pharmacol* **140**:173–179.

Gao X, Xie C, Wang Y, Luo Y, Yagai T, Sun D, Qin X, Krausz KW, and Gonzalez FJ (2016) The antiandrogen flutamide is a novel aryl hydrocarbon receptor ligand that disrupts bile acid homeostasis in mice through induction of Abcc4. *Biochem Pharmacol* **119**:93–104.

Guyot E, Chevallier A, Barouki R, and Coumoul X (2013) The AhR twist: ligand-dependent AhR signaling and pharmaco-toxicological implications. *Drug Discov Today* **18**:479–486.

Haarmann-Stemmann T, Sendker J, Götz C, Krug N, Bothe H, Fritsche E, Proksch P, and Abel J (2010) Regulation of dioxin receptor function by different beta-carboline alkaloids. *Arch Toxicol* **84**:619–629.

Hahn ME (2002) Aryl hydrocarbon receptors: diversity and evolution. *Chem Biol Interact* **141**:131–160.

Han EH, Kim HG, Im JH, Jeong TC, and Jeong HG (2009) Up-regulation of CYP1A1 by rutaecarpine is dependent on aryl hydrocarbon receptor and calcium. *Toxicology* **266**:38–47.

Jeon TW, Jin CH, Lee SK, Jun IH, Kim GH, Lee DJ, Jeong HG, Lee KB, Jahng Y, and Jeong TC (2006) Immunosuppressive effects of rutaecarpine in female BALB/c mice. *Toxicol Lett* **164**:155–166.

Jiang C, Xie C, Lv Y, Li J, Krausz KW, Shi J, Brocker CN, Desai D, Amin SG, Bisson WH, et al. (2015) Intestine-selective farnesoid X receptor inhibition improves obesity-related metabolic dysfunction. *Nat Commun* **6**:10166–10183.

Kawano Y, Nishiumi S, Tanaka S, Nobutani K, Miki A, Yano Y, Seo Y, Kutsumi H, Ashida H, Azuma T, et al. (2010) Activation of the aryl hydrocarbon receptor induces hepatic steatosis via the upregulation of fatty acid transport. *Arch Biochem Biophys* **504**:221–227.

Ko HC, Wang YH, Liou KT, Chen CM, Chen CH, Wang WY, Chang S, Hou YC, Chen KT, Chen CF, et al. (2007) Anti-inflammatory effects and mechanisms of the ethanol extract of Evodia rutaecarpa and its bioactive components on neutrophils and microglial cells. *Eur J Pharmacol* **555**:211–217.

Köhle C and Bock KW (2007) Coordinate regulation of Phase I and II xenobiotic metabolisms by the Ah receptor and Nrf2. *Biochem Pharmacol* **73**:1853–1862.

Liao CH, Pan SL, Guh JH, Chang YL, Pai HC, Lin CH, and Teng CM (2005) Antitumor mechanism of evodiamine, a constituent from Chinese herb Evodiae fructus, in human multiple-drug resistant breast cancer NCI/ADR-RES cells in vitro and in vivo. *Carcinogenesis* **26**:968–975.

Lin S, Ren L, and Sun A (2015) Acute toxicity study on evodiamine, rutacarpine and evodia total alkaloids in mice. *J Zunyi Med Univ* **38**:146–149.

Nebert DW and Karp CL (2008) Endogenous functions of the aryl hydrocarbon receptor (AHR): intersection of cytochrome P450 1 (CYP1)-metabolized eicosanoids and AHR biology. *J Biol Chem* **283**:36061–36065.

Park CH, Kim SH, Choi W, Lee YJ, Kim JS, Kang SS, and Suh YH (1996) Novel anticholinesterase and antiamnesic activities of dehydroevodiamine, a constituent of Evodia rutaecarpa. *Planta Med* **62**:405–409.

Perkins A, Phillips JL, Kerkvliet NI, Tanguay RL, Perdew GH, Kolluri SK, and Bisson WH (2014) A structural switch between agonist and antagonist bound conformations for a ligand-optimized model of the human aryl hydrocarbon receptor ligand binding domain. *Biology (Basel)* **3**:645–669.

Qi Z, Qian Z, and Jin RM (2011) Time-effect and dose-effect of Evodia rutaecarpa on hepatotoxicity in mice. *Zhongguo Shiyan Fangjixue Zazhi* **17**:232–237.

Schmidt JV, Su GH, Reddy JK, Simon MC, and Bradfield CA (1996) Characterization of a murine Ahr null allele: involvement of the Ah receptor in hepatic growth and development. *Proc Natl Acad Sci USA* **93**:6731–6736.

Seglen PO (1976) Preparation of isolated rat liver cells. *Methods Cell Biol* **13**:29–83.

Shang RF, Wang GH, Xu XM, Liu SJ, Zhang C, Yi YP, Liang JP, and Liu Y (2014) Synthesis and biological evaluation of new pleuromutilin derivatives as antibacterial agents. *Molecules* **19**: 19050–19065.

Sheu JR, Hung WC, Wu CH, Lee YM, and Yen MH (2000) Antithrombotic effect of rutaecarpine, an alkaloid isolated from Evodia rutaecarpa, on platelet plug formation in in vivo experiments. *Br J Haematol* **110**:110–115.

Shimizu Y, Nakatsuru Y, Ichinose M, Takahashi Y, Kume H, Mimura J, Fujii-Kuriyama Y, and Ishikawa T (2000) Benzo[a]pyrene carcinogenicity is lost in mice lacking the aryl hydrocarbon receptor. *Proc Natl Acad Sci USA* **97**:779–782.

Sorg O (2014) AhR signalling and dioxin toxicity. *Toxicol Lett* **230**:225–233.

Spink BC, Bloom MS, Wu S, Sell S, Schneider E, Ding X, and Spink DC (2015) Analysis of the AHR gene proximal promoter GGGGC-repeat polymorphism in lung, breast, and colon cancer. *Toxicol Appl Pharmacol* **282**:30–41.

Stejskalova L, Dvorak Z, and Pavek P (2011) Endogenous and exogenous ligands of aryl hydrocarbon receptor: current state of art. *Curr Drug Metab* **12**:198–212.

Ueng YF, Wang JJ, Lin LC, Park SS, and Chen CF (2001) Induction of cytochrome P450-dependent monooxygenase in mouse liver and kidney by rutaecarpine, an alkaloid of the herbal drug Evodia rutaecarpa. *Life Sci* **70**:207–217.

Veldhoen M, Hirota K, Christensen J, O'Garra A, and Stockinger B (2009) Natural agonists for aryl hydrocarbon receptor in culture medium are essential for optimal differentiation of Th17 T cells. *J Exp Med* **206**:43–49.

Wang M, Chen L, Liu D, Chen H, Tang DD, and Zhao YY (2017) Metabolomics highlights pharmacological bioactivity and biochemical mechanism of traditional Chinese medicine. *Chem Biol Interact* **273**:133–141.

Yang S (1998) A translation of the Shen Nong Ben Cao Jing. pp. 1–189, Blue Poppy Press, Boulder, CO.

Yang XW (2008) Toxicological assessment on safety of water and 70% ethanolic extracts of nearly ripe fruit of Evodia rutaecarpa. *Zhongguo Zhong Yao Za Zhi* **33**:1317–1321.

Yang XW and Tang J (2007) Chemical constituents of the unripe fruits of Evodia rutaecarpa. *J Chin Pharm Sci* **16**:20–23.

Yang Y, Zhang L, Zhang Y, and Yang X (2017) Simultaneous assessment of absorption characteristics of coumarins from Angelicae Pubescentis Radix: in vitro transport across Caco-2 cell and in vivo pharmacokinetics in rats after oral administration. *J Chromatog* **1060**:308–315.

Yang XW, Teng J, Wang Y, and Xu W (2009) The permeability and the efflux of alkaloids of the Evodiae fructus in the Caco-2 model. *Phytother Res* **23**:56–60.

Yu H, Jin H, Gong W, Wang Z, and Liang H (2013) Pharmacological actions of multi-target-directed evodiamine. *Molecules* **18**:1826–1843.

Yu H, Tu Y, Zhang C, Fan X, Wang X, Wang Z, and Liang H (2010) Evodiamine as a novel antagonist of aryl hydrocarbon receptor. *Biochem Biophys Res Commun* **402**:94–98.

Zhang A, Sun H, Wang Z, Sun W, Wang P, and Wang X (2010a) Metabolomics: towards understanding traditional Chinese medicine. *Planta Med* **76**:2026–2035.

Zhang H, Yang XW, and Chui YX (1999) Complete assignment of 1H and 13C NMR chemical shifts of evodiamine, rutarcarpine, and dehdroevodiamine. *Chin J Magnet Reson* **16**:563–568.

Zhang L, Hatzakis E, Nichols RG, Hao R, Correll J, Smith PB, Chiaro CR, Perdew GH, and Patterson AD (2015) Metabolomics reveals that aryl hydrocarbon receptor activation by environmental chemicals induces systemic metabolic dysfunction in mice. *Environ Sci Technol* **49**:8067–8077.

Zhang Q, Xu G, Wu L, Ma X, Zeng Z, Huang L, Yu R, and Liu H (2010b) Preliminary study of metabonomcs on aqueous extract of Evodia rutaecarpa in sprague-dawley rats. *Zhongguo Zhong Yao Za Zhi* **35**:99–102.

Zhang Q, Zhou Q, Jin RM, Yao GT, and Chen XM (2011) Preliminary study on hepatotoxicity and nephrotoxicity induced by rutaecarpine. *Chin J Exper Tradit Med Form* **17**:221–225.

Zhang YT, Li Z, Zhang K, Zhang HY, He ZH, Xia Q, Zhao JH, and Feng NP (2017) Co-delivery of evodiamine and rutaecarpine in a microemulsion-based hyaluronic acid hydrogel for enhanced analgesic effects on mouse pain models. *Int J Pharm* **528**:100–106.

Address correspondence to: Frank J. Gonzalez, Laboratory of Metabolism, Center for Cancer Research, National Cancer Institute, National Institutes of Health, 37/3106, 9000 Rockville Pike, Bethesda, MD 20892. E-mail: gonzalef@mail.nih.gov; or Xiuwei Yang, State Key Laboratory of Natural and Biomimetic Drugs and Department of Natural Medicines, School of Pharmaceutical Sciences, Peking University, Beijing, 100191, China. E-mail: xwyang@bjmu.edu.cn